



OPEN

## Pile caps with inclined shear reinforcement and steel fibers

Aaron Nzambi<sup>1</sup>✉, Lana Gomes<sup>1</sup>, Cledinei Amanajás<sup>1</sup>, Francisco Silva<sup>2</sup> & Dênio Oliveira<sup>1</sup>

This experimental investigation presents results and a discussion on a series of four reinforced concrete pile caps with and without steel fibers, measuring  $400 \times 400 \times 1000 \text{ mm}^3$ , which were tested under concentric loading. The study set the steel fiber and the inclined shear reinforcement as variables. The fiber volume fraction was 1.5%, and the concrete compressive strength was 25 MPa. The results showed a tendency to increase ductility and ultimate strength with the use of inclined shear reinforcement; the same behavior was observed with the addition of steel fibers, improving the performance of the tested pile caps. This study opens the possibility of designing slender pile caps, especially when associated with both analyzed parameters.

Foundations are among the most important structural elements used for load transfer from a building to piles or caissons. Pile caps can be classified as rigid or flexible based on criteria similar to those used for shallow foundations. Therefore, the larger and more rigid the structure is, the more complex its design becomes. According to NBR 6118<sup>1</sup>, rigid pile caps are not prone to diagonal tension failure; most often, failure occurs in compression struts<sup>2</sup>. However, some doubt remains as to whether this behavior can be modified with strut strengthening. In the literature, studies<sup>3–5</sup> have suggested limiting the height of the block as a function of the angle of inclination of the strut, ranging from  $45^\circ$  to  $55^\circ$ ; this may result in an overdesign of the structure. Fighting the shear cracks through reinforcement mechanisms that can improve the performance of the blocks is an ideal way to optimize the design and safety of such structural elements. This can be achieved by using shear reinforcement and/or steel fibers to improve the mechanical properties of concrete in terms of shear, compression, and flexure; in addition, steel fiber reinforced concrete (SFRC) enhances performance in energy absorption, cracking control, and ductility<sup>6,7</sup>. The use of SFRC is being expanded, and its applications range from floor pavements to special structural elements or those subjected to an aggressive or corrosive environment without affecting their durability<sup>8</sup>.

Thus, this experimental study explores the effectiveness of inclined reinforcement and the contribution of steel fibers in improving the performance of concrete pile caps subjected to shear forces since, economically, a considerable gain in strength increase can make this approach feasible and decrease the volume of concrete in pile caps.

### Calculation model

In the present study, the pile caps were designed using the strut-and-tie method (STM), which is the most widespread calculation model for the design of rigid pile caps. This design is based on the experimental works previously developed by Blénot and Frémy<sup>4</sup>. The model consists of designing a spatial truss inside a pile cap using tension and compression bars that are connected through nodes, as shown in Fig. 1.

The effective depth ( $d$ ) of the pile cap is given by Eq. 1. To ensure adequate structural behavior of the pile cap, Blénot and Frémy<sup>4</sup> recommended that  $\theta$  should be within a  $45^\circ \leq \theta \leq 55^\circ$  range. For the minimum spacing between the piles adopted in the work, the distance  $L$  was equal to three times the edge distance of the pile ( $D$ ), according to the recommendations of Moraes<sup>9</sup>, ( $L \geq 3 \cdot D$ ).

$$d = \tan \theta \cdot (0.5 \cdot L - 0.25 \cdot a_c) \quad (1)$$

where  $L$  is the spacing between piles;  $a_c$  is the larger side of the column.

The determinations of the acting stresses near the column and the pile are calculated through Eqs. (2) and (3), respectively. The equations also define the normative verification limits for the design.

$$\sigma_{u,tc} = \frac{F_d}{A_c \cdot \sin^2 \theta} \leq 1.4 \cdot f_c \quad (2)$$

<sup>1</sup>Department of Civil Engineering, Federal University of Pará, Belém, PA 66075-110, Brazil. <sup>2</sup>Department of Civil Engineering, University of Amazônia, Belém, PA 66065-205, Brazil. ✉email: aaronkadima@gmail.com

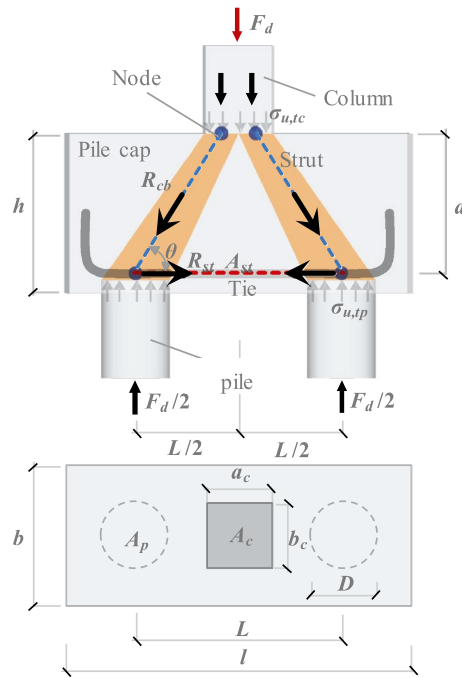


**Figure 1.** Strut-and-tie model for a two-pile cap (Note:  $F_d/2$  is the column load for a pile;  $R_{ct}$  is the compressive force on the strut;  $R_{st}$  is the tensile force on the tie;  $\theta$  is the angle of inclination of the strut).

$$\sigma_{u,tp} = \frac{F_d}{2 \cdot A_p \cdot \sin^2\theta} \leq 0.85 \cdot f_c \tag{3}$$

where  $\sigma_{u,tc}$  and  $\sigma_{u,tp}$  represent the failure stresses of the strut in the regions of the column and the pile, respectively;  $A_c$  and  $A_p$  are the cross-sectional areas of the column and the pile, respectively;  $F_d$  is the design load; and  $f_c$  is the concrete compressive strength.

The longitudinal reinforcement area of the tie over the piles was calculated according to Eq. (4). Equation (5), proposed by Delalibera and Giongo<sup>10</sup>, was used to calculate the tensile force in the tie.

$$A_{st} = \frac{R_{st}}{f_{ys}} \tag{4}$$

$$R_{st} = \frac{F_d \cdot (2L - a_c)}{8 \cdot d} \tag{5}$$

where  $A_{st}$  is the total area of longitudinal steel reinforcement in the tie,  $R_{st}$  is the tensile force on the tie, and  $f_{ys}$  is the yield strength of the longitudinal steel reinforcement.

### Experimental setup

**Materials and methods.** Cement, coarse aggregate, fine aggregate, and water–cement ratio ( $w/c$ ) were mixed in a 1:2.90:2.10:0.55 proportion. Superplasticizer additive was used to maintain the constant workability of concrete. Table 1 lists the constituents used for the mixtures, and Table 2 lists the mechanical properties of the crimped steel fiber. Flat crimped type C fiber (Fig. 2), classified according to NBR 15530<sup>11</sup>, was used in this research because, according to Soroushian and Bayasi<sup>12</sup> and Mahakavi and Chithra<sup>13</sup>, hooked-end and crimped fibers are more effective at improving the performance of structural elements as a result of their additional anchoring mechanisms<sup>14</sup>. The concrete test specimens were molded and cured for 28 days in the laboratory with 85% relative air humidity. Table 3 presents the results of the characterization tests at 7, 14, and 28 days. There was no significant difference between the plain concrete and the concrete with fiber, so average values were adopted for both mixtures: 25.8 MPa, 1.9 MPa, and 28.4 GPa, respectively, for compressive strength ( $f_c$ ), tensile strength ( $f_{ct}$ ), and modulus of elasticity ( $E_c$ ).

The steel bars used in the tests were classified according to NBR 7480<sup>15</sup>. Their mechanical properties were determined through axial tensile tests, following the recommendations of NBR ISO 6892-1<sup>16</sup>. Three samples were used in the tensile test; the test bars measured 5.0 mm, 10.0 mm and 12.5 mm in diameter and were used in the stirrups, inclined shear reinforcement and flexural reinforcement, respectively. Table 4 presents the mechanical properties of the steel used.

Constituents	Type	$\rho$ (kg/m <sup>3</sup> )	Weight per unit volume (kg)	
			Mixture 1	Mixture 2
Cement	Portland CII-Z-32RS	3100	269.52	269.52
Small aggregate	Sand (avg. 2.7 mm)	2830	781.62	781.62
Large aggregate	Coarse aggregates (d <sub>max</sub> = 10 mm)	2600	566.00	566.00
Fiber	Crimped steel fiber	7850	–	85.84*
Admixture	Superplasticizer	–	–	–
Water	pH < 9	1000	148.24	148.24

**Table 1.** Composition of concrete. w/c = 0.55 for all mixtures and slump test workability 140 mm; \* $V_f = 1.5\% = 117.75 \text{ kg/m}^3$ ,  $C_f = V_c \times V_f = 0.729 \text{ m}^3 \times 117.75 \text{ kg/m}^3 = 85.84 \text{ kg}$ ;  $\rho$  is the density;  $C_f$  is the fiber consumption;  $V_c$  is the volumetric fraction of the concrete; and  $V_f$  is the volumetric fraction of the fiber.

$d_f$ (mm)	$l_f$ (mm)	$l_f/d_f$	$f_{u,f}$ (MPa)	$E_f$ (GPa)
~ 1.0	38.0	38.00	900.00	200.00

**Table 2.** Mechanical properties of crimped steel fibers.  $d_f$  = equivalent diameter of fiber;  $l_f$  = fiber length;  $l_f/d_f$  = aspect ratio;  $f_{u,f}$  = ultimate tensile strength of fiber; and  $E_f$  = elastic modulus of fiber.

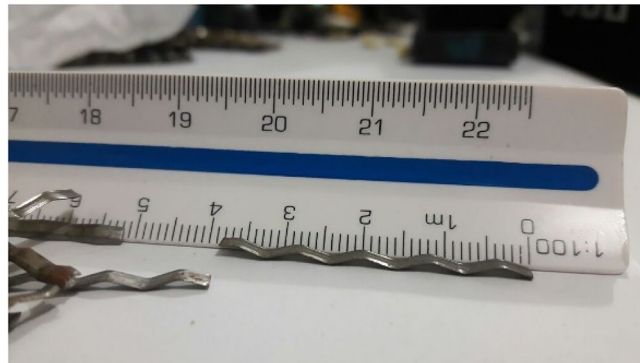


**Figure 2.** Flat crimped steel fiber. (Reprinted with permission from Nzambi et al.<sup>14</sup>.)

Age of concrete (Days)	Number of cylindrical specimens	$f_{c,m}$ (MPa)	$f_{ct,m}$ (MPa)	$E_c$ (GPa)
07	3	14.30	1.24	21.18
14		16.90	1.38	23.02
28		25.80	1.90	28.44

**Table 3.** Results for characterization of concrete (avg. values).

$\varnothing_s$ (mm)	$\varepsilon_{ys}$ (‰)	$f_{ys}$ (MPa)	$f_{us}$ (MPa)	$E_s$ (GPa)	Location
5.0	4.63	529.50	550.00	201.70	Stirrups
10.0	2.42	500.00	556.00	206.61	Inclined shear reinforcement
12.5	3.05	610.30	716.00	200.00	longitudinal reinforcement

**Table 4.** Mechanical properties of the reinforcements used.  $\varnothing_s$  = steel bar diameter;  $\varepsilon_{ys}$  = strains;  $f_{ys}$  = yield stresses;  $f_{us}$  = ultimate tensile strength of steel bar;  $E_s$  = modulus of elasticity.

Pile cap	$a_c$ (mm)	$d$ (mm)	$b$ (mm)	$h$ (mm)	$l$ (mm)	$L$ (mm)	$V_f$ (%)	Inclined shear reinforcement
PC01 <sub>REF</sub>	200	350	400	400	1000	600	–	–
PC02 <sub>SFRC</sub>							–	–
PC03 <sub>SFRC+IR</sub>							1.5	Yes
PC04 <sub>IR</sub>							–	–

**Table 5.** General characteristics of the pile caps. NOTE: REF = reference (plain concrete); SFRC = steel fiber reinforcement concrete; and IR = inclined reinforcement.

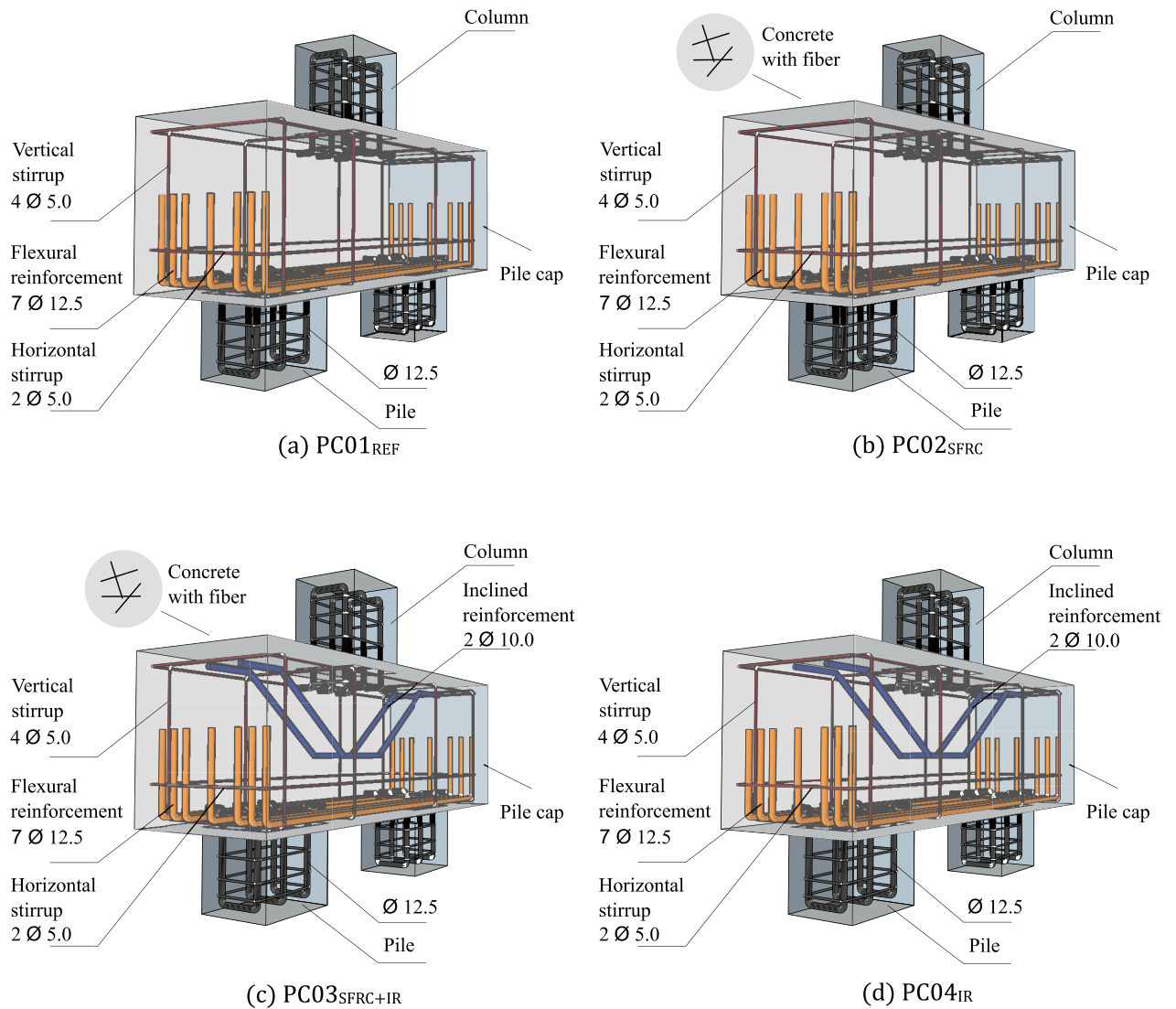


**Figure 3.** Details of the two-pile caps.

**Characteristics of the samples.** The design of the pile caps followed the strut-and-tie method presented in “Calculation model” section<sup>4</sup>. The dimensions were constant for all pile caps, as shown in Table 5. The column located on the upper surface of the piles had a cross-section of  $200 \times 200$  mm<sup>2</sup> with a height of 250 mm. The piles had the same dimensions for the cross section, but their height was 200 mm (Figs. 3, 4). The compressive strength of the concrete was 25.8 MPa for all pile caps mixtures. The longitudinal reinforcement and horizontal and vertical stirrups were the same. Pile caps PC03<sub>SFRC+IR</sub> and PC04<sub>IR</sub> were made with two inclined bars with a diameter of 10.0 mm. The spacing between the bars was 100 mm, and each bar had a length of 1000 mm. The following are the other characteristics of each pile cap:

- PC01<sub>REF</sub>: concrete cast without the addition of steel fiber and inclined shear reinforcement, as shown in Fig. 3a;

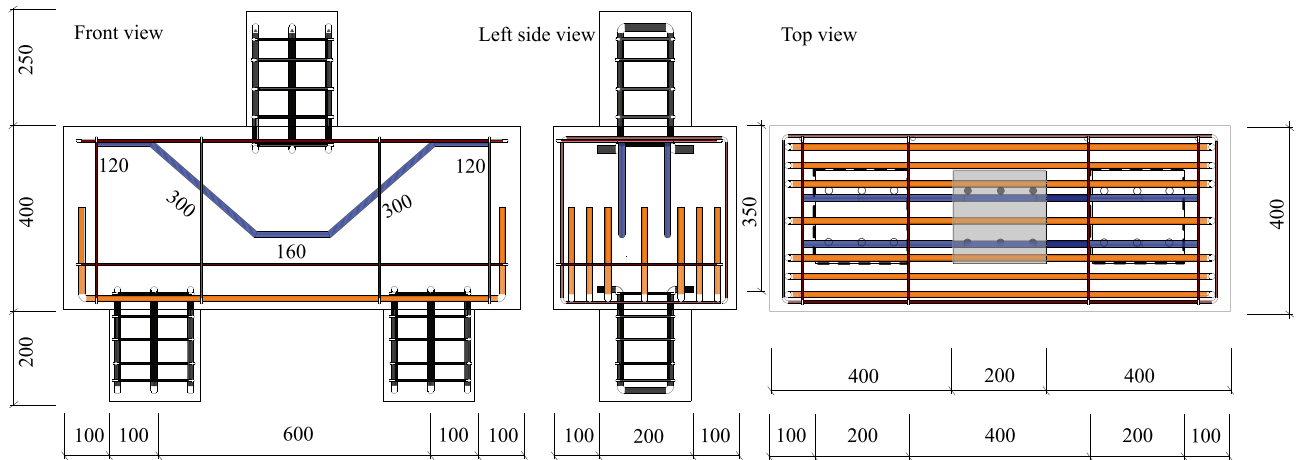


**Figure 4.** Pile cap dimensions (in mm).

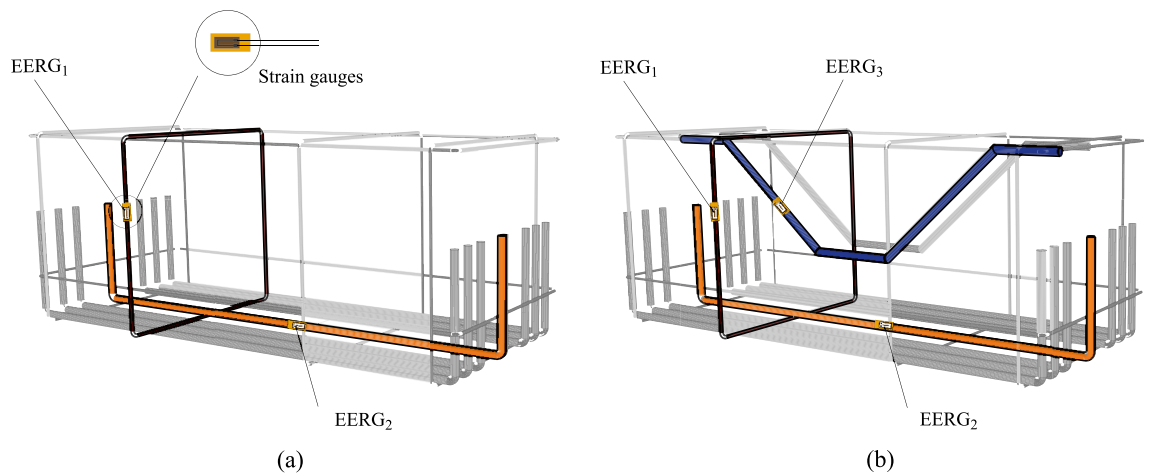


**Figure 5.** Position of strain gauges on the reinforcements: (a) for PC01<sub>REF</sub> and PC04<sub>IR</sub> and (b) for PC02<sub>SFRC</sub> and PC03<sub>SFRC+IR</sub>.

- PC02<sub>SFRC</sub>: concrete cast with the addition of steel fiber ( $V_f = 1.5\%$ ) but without inclined shear reinforcement, as shown in Fig. 3b;
- PC03<sub>SFRC+IR</sub>: concrete characteristic equal to PC02<sub>SFRC</sub> + inclined shear reinforcement, as shown in Fig. 3c;
- PC04<sub>IR</sub>: concrete characteristic equal to PC01<sub>REF</sub> but with inclined shear reinforcement, as shown in Fig. 3d.

**Instrumentation.** The strains in the steels were measured using electrical resistance strain gauges (EESG, EXCEL Sensors, PA-06-125AA-120L), positioned as shown in Fig. 5. Therefore, one strain gauge was installed in the middle of the central flexural reinforcement bar, one in the inclined shear reinforcement bar, and one in the vertical stirrup at the level of the point of intersection with the inclined reinforcement (Fig. 6a), to be in the same stress line caused by the compression strut. The vertical displacements were measured using a deflectometer placed at the bottom of the pile caps at a distance of  $l/2 = 500$  mm, as shown in Fig. 6b. Figure 7 shows the final aspect of the pile caps ready for testing.

**Test setup.** All pile caps were subjected to centered loading and applied on the face of the column. The test setup was composed of a hollow hydraulic jack and a hydraulic pump (Enerpac). Both the jack and the pump had a 1000 kN capacity, a digital load cell for 1000 kN, a precision of 500 N and an Amsler testing machine used as the gantry system. Figure 8 shows the test system. In all test specimens, an initial load was applied to eliminate looseness.

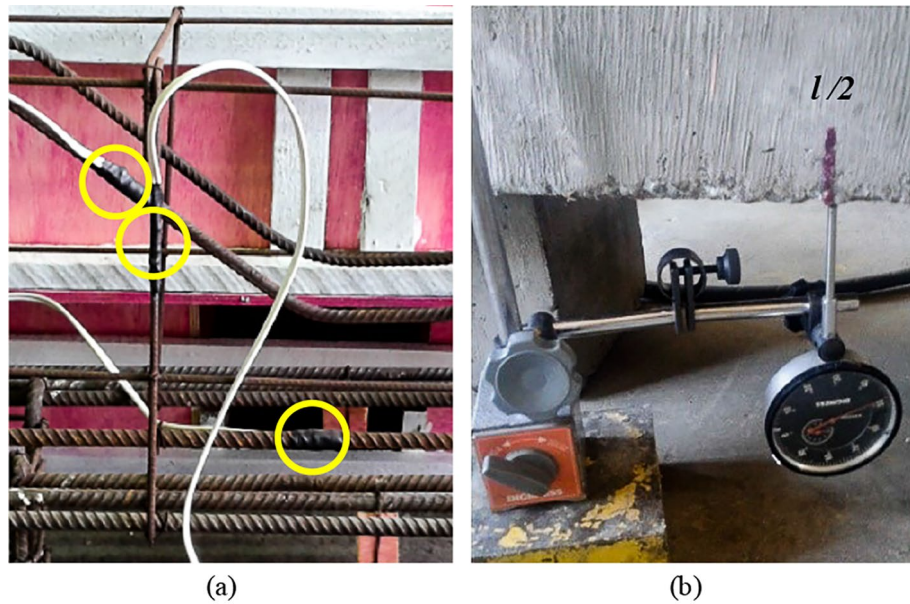


**Figure 6.** Instrumentation: (a) installed strain gauges and (b) deflectometer placement.



**Figure 7.** Pile cap specimens.

## Results and discussion

Table 6 presents the results of the experimental bearing capacity. In terms of strength gain, PC02<sub>SFRC</sub> and PC04<sub>IR</sub> presented an increase in the ultimate strength of approximately 40% compared to block PC01<sub>REF</sub>. Furthermore, the fibers increased the load-bearing capacity of the PC03<sub>SFRC+IR</sub> pile cap by 7% when used with inclined reinforcement compared to PC04<sub>IR</sub>.

**Load–displacement ratio and tenacity.** This study focused only on the displacement in the center of the pile caps ( $l/2 = 500$  mm); this way, the analyses were made based on the load–displacement ( $V - \delta$ ) ratio and the quantities that characterize this ratio. Although PC02<sub>SFRC</sub> and PC04<sub>IR</sub> had almost the same ultimate strength, Table 7 and Fig. 9 show a slight decrease in displacements with the addition of steel fiber; this effect was more pronounced with PC03<sub>SFRC+IR</sub>, which showed lower displacements, at a 20%, and 44% reduction, respectively, compared to PC01<sub>REF</sub> and PC04<sub>IR</sub>.

An analysis was made of tenacity ( $T_E$ ), that is, the capacity of the pile caps to absorb strain energy (Table 7), based on the  $T_{E,Pilecaps}/T_{E,REF}$  ratio. Clearly, the fibers and the inclined reinforcement helped to improve the tenacity of the pile caps; however, the most relevant values in terms of  $T_E$  were found for PC04<sub>IR</sub>, with  $T_{E,Pilecaps}/T_{E,REF} = 3.35$ , where  $T_{E,Pilecaps}$  and  $T_{E,REF}$  were the tenacity of the pile caps with some type of additional reinforcement and the reference tenacity, respectively. In terms of displacement, the gains of the pile caps with SFRC and inclined shear reinforcement were not so substantial, mainly for PC03<sub>SFRC+IR</sub> (with hybrid reinforcement). It is assumed that the steel fibers inhibited the action of the inclined shear reinforcement, and for this reason, the

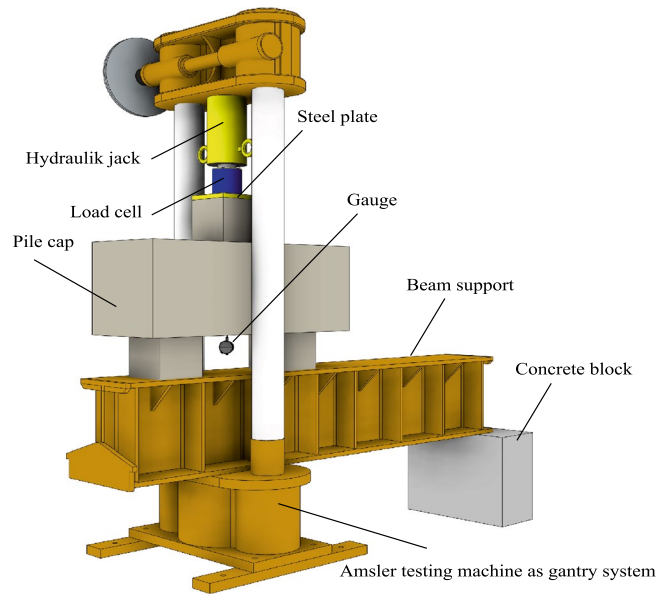


**Figure 8.** Test setup.

Pile cap	Strut angle, $\theta$ (°)	Experimental	
		Ultimate failure Load, $V_u$ (kN)	Strength increase, $V_{u,Pilecaps}/V_{u,REF}$ (%)
PC01 <sub>REF</sub>	54.46*	489.00	–
PC02 <sub>SFRC</sub>		680.00	39
PC03 <sub>SFRC+IR</sub>		720.00	47
PC04 <sub>IR</sub>		685.00	40

**Table 6.** Ultimate failure loads observed during testing.  $V_{u,Pilecaps}$  = failure loads of the pile caps with steel fibers and/or inclined reinforcement  $V_{u,REF}$  = failure loads of the pile caps without steel fibers and/or inclined reinforcement. \*From Eq. (1),  $\tan \theta = d/(0.5 \cdot L - 0.25 \cdot a_c) = 350/(0.25 \cdot 600 - 0.25 \cdot 200) = 1.4 \rightarrow \arctan \theta = 54.46$ .

Pile cap	$V_u$ (kN)	$\delta_u$ (mm)	$T_E$ (kJ)	$\delta_{u,Pilecaps}/\delta_{u,REF}$	$T_{E,Pilecaps}/T_{E,REF}$
PC01 <sub>REF</sub>	489.00	3.28	3.62	–	–
PC02 <sub>SFRC</sub>	680.00	3.47	7.02	1.06	1.94
PC03 <sub>SFRC+IR</sub>	720.00	2.61	10.02	0.80	2.77
PC04 <sub>IR</sub>	685.00	3.93	12.14	1.20	3.35

**Table 7.** Parameters defining the  $V - \delta$  ratio.

results of that pile cap were below expectations in terms of ductility. However, this structural element clearly had major strength gains. Finally, it should be noted that for PC04<sub>IR</sub>, the  $\delta_{u,Pilecaps}/\delta_{u,REF}$  ratio = 1.20 was more significant.

**Mobilization of the flexural reinforcement.** Table 8 shows the maximum strains of the flexural reinforcement  $\epsilon_{fu}$ , as expressed in the load–strain ratio. This information enables the analysis of the  $\epsilon_{fu,Pilecaps}/\epsilon_{fu,REF}$  ratio and the angular constant  $k$ . The angular constant, determined by  $k = V/\epsilon_f$ , evaluates the tangent of the slope angle of the linear portion of the  $V - \epsilon_f$  ratio. The  $\epsilon_{fu,Pilecaps}/\epsilon_{fu,REF}$  ratio shows that the hybrid use of SFRC with inclined reinforcement (PC03<sub>SFRC+IR</sub>) had the best performance compared to PC01<sub>REF</sub>; that is, the increase in fiber consumption strengthened the reinforcement under tensile stress since the pile caps with SFRC had  $\epsilon_{fu,Pilecaps}/\epsilon_{fu,REF} \in [0.9-1.3]$ . Moreover, in general, there was no yield stress in the reinforcements monitored in the pile caps, with  $\epsilon_{fu} < \epsilon_{sy} = 3.05 \text{ ‰}$  (Fig. 10). The evaluation of the angular constant shows that the responses in the elastic phase are within normal limits for the values presented, at  $k \in [4000-10000]$ .

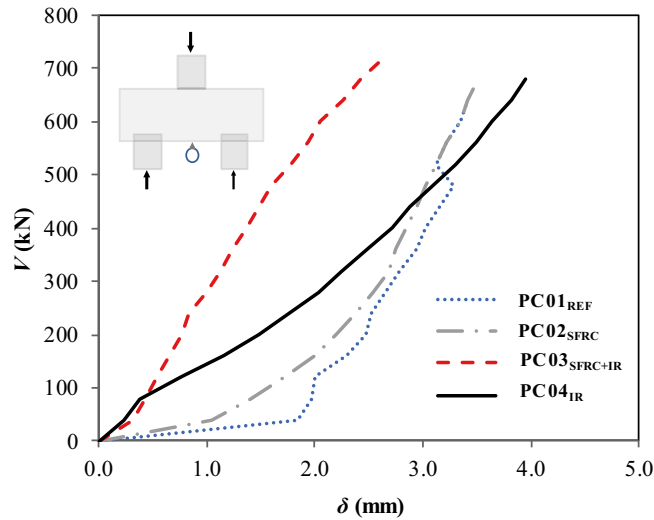


Figure 9. Load–displacement ratio.

Pile cap	$V_u$ (kN)	$\epsilon_{fu}$ (‰)	$k$	$\epsilon_{fu, pilecaps} / \epsilon_{fu, REF}$	Failure mode
PC01 <sub>REF</sub>	489.00	0.74	4090.9	–	Shear
PC02 <sub>SFRC</sub>	680.00	0.68	6153.9	0.92	
PC03 <sub>SFRC+IR</sub>	720.00	0.95	4500.0	1.28	
PC04 <sub>IR</sub>	685.00	0.10	10,000.0	0.14	

Table 8. Parameters that define the  $V - \epsilon_f$  ratio.

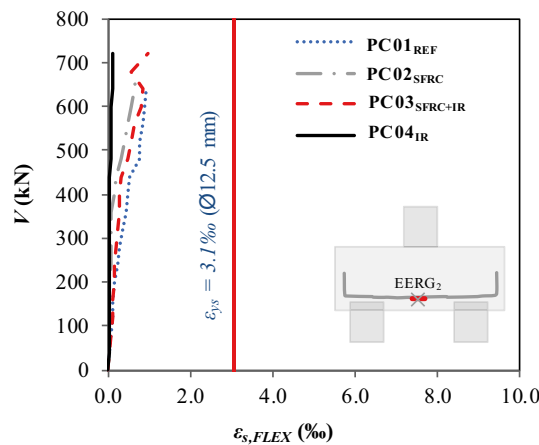
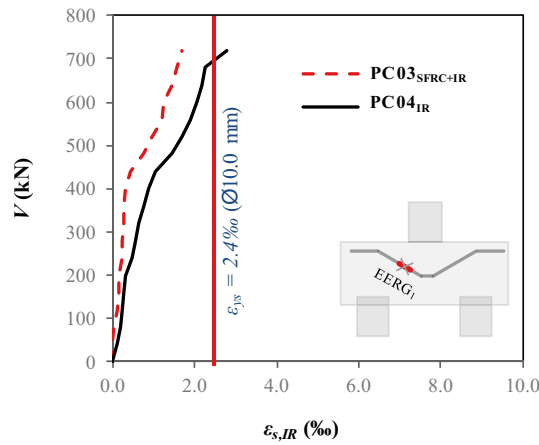


Figure 10. Load–strain ratio of the flexural reinforcement.

**Mobilization of the inclined shear reinforcement.** On this occasion, only pile caps PC03<sub>SFRC+IR</sub> and PC04<sub>IR</sub> were analyzed, as they have inclined shear reinforcement. In Fig. 11, the results show that strain in the instrumented reinforcement of PC04<sub>IR</sub> was higher than yield strain, with  $\epsilon_{st, IR} > \epsilon_{sy} = 2.42\%$ . However, for the pile cap with hybrid composition (fibers + inclined reinforcement), the inclined reinforcement did not have yield stress. This finding suggests that the steel fibers assumed the function of reinforcement and inhibited the strain of the inclined reinforcement. In summary, the results indicate that the use of inclined shear reinforcement together with steel fibers can lead to oversizing, i.e., the fiber restricts the action of the reinforcement and vice versa. In addition, the pile caps had similar gains in strength, ductility and tenacity, with the exception of the reference pile cap; that is, it is hardly practical and economical to use steel fibers together with inclined shear reinforcement.





**Figure 11.** Load–strain ratio of the inclined reinforcements.

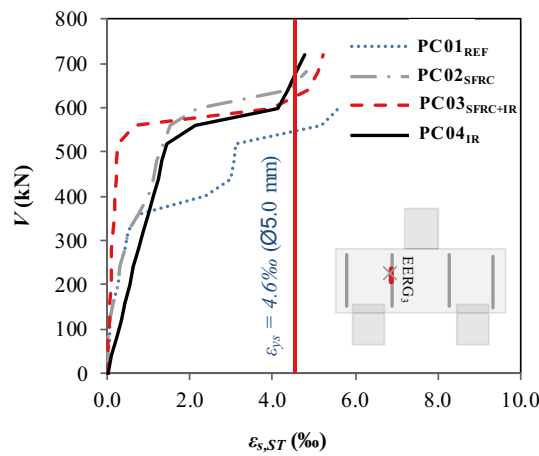


**Figure 12.** Load–strain ratio of the stirrups.

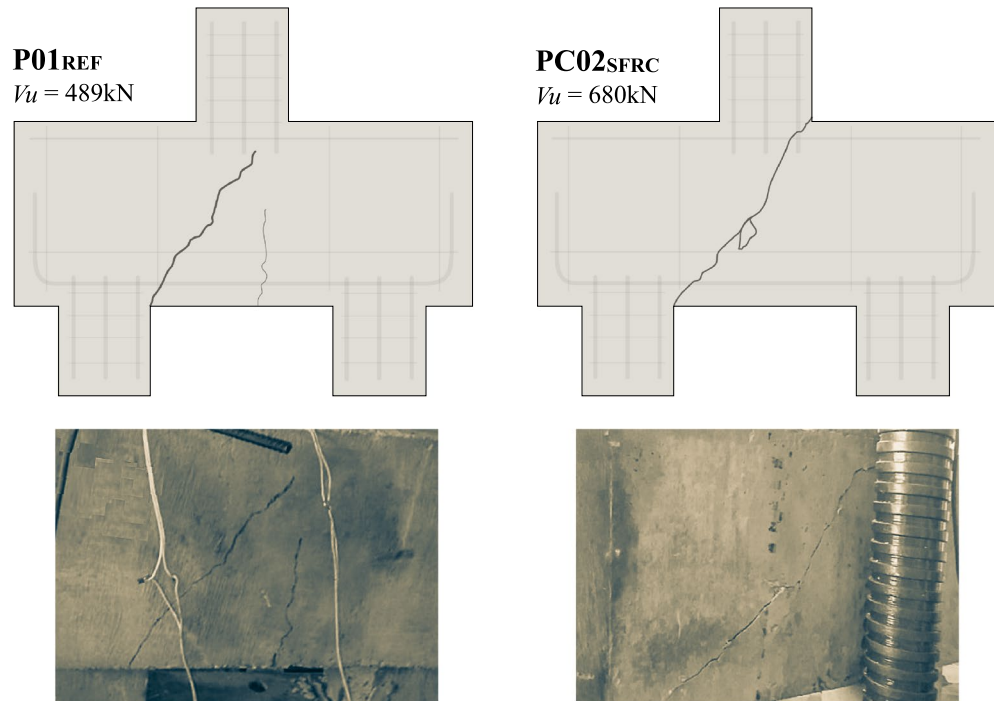
Pile cap	$V_u$ (kN)	$\epsilon_{su}$ (‰)	$V_{2L}$ (kN)	$\epsilon_{s2L}$ (‰)	$\epsilon_{su,Pilecaps}/\epsilon_{su,REF}$	$V_{2L,Pilecaps}/V_{2L,REF}$	$\epsilon_{s2L,Pilecaps}/\epsilon_{s2L,REF}$
PC01 <sub>REF</sub>	489.00	5.65	320.00	0.51	–	–	–
PC02 <sub>SFRC</sub>	680.00	4.85	320.00	0.52	0.86	1.00	1.02
PC03 <sub>SFRC+IR</sub>	720.00	5.25	520.00	0.24	0.93	1.63	0.47
PC04 <sub>IR</sub>	685.00	4.75	510.00	1.50	0.84	1.59	2.94

**Table 9.** Characterization of the  $V - \epsilon_s$  ratio.

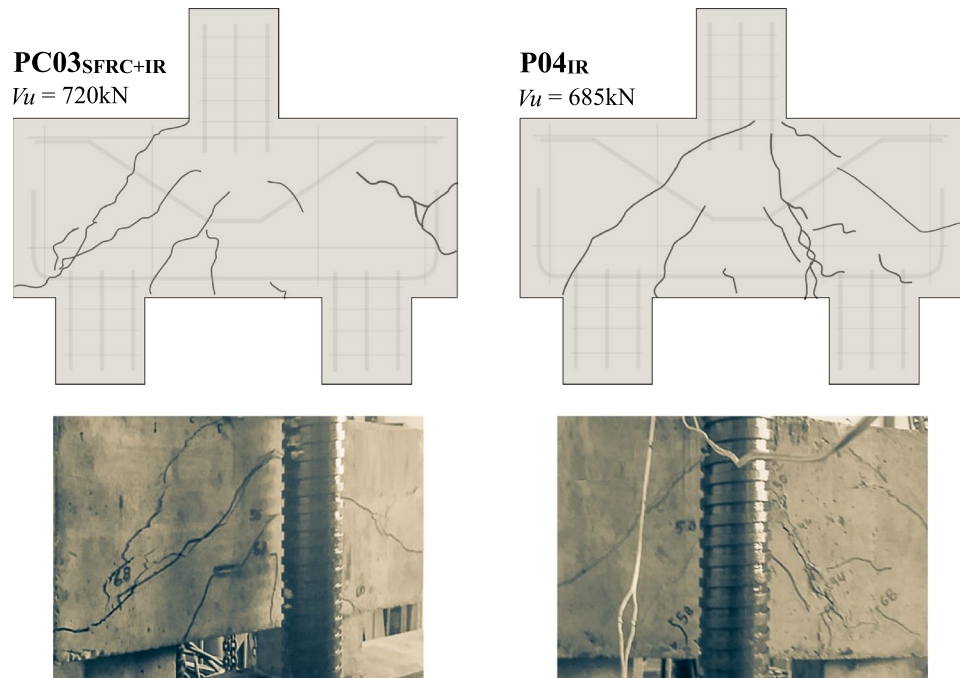
**Mobilization of the stirrups.** The analysis of stirrup mobilization was based on the results shown in the load–strain graph,  $V - \epsilon$  (Fig. 12). The graph shows that, in general, the results had different bilinear behaviors, since one section represents the elastic phase (without the appearance of diagonal cracks), while the second section corresponds to the beginning and progress of shear cracks.

Table 9 shows the coordinates that define the ultimate load ( $V_u - \epsilon_{su}$ ) as well as the coordinate indicating the start of the second linear section ( $V_{2L} - \epsilon_{s2L}$ ). The result for strain  $\epsilon_{su}$  shows that yield stress occurred in the transverse reinforcement of all pile caps,  $\epsilon_{su} > \epsilon_{sy} = 4.63$  ‰. The  $\epsilon_{su,Pilecaps}/\epsilon_{su,REF}$  ratio clearly shows that the level of strain in the stirrups of the pile caps with additional reinforcement (steel fibers and/or inclined reinforcement) is lower than the level of the reference pile cap, namely,  $\epsilon_{su,Pilecaps}/\epsilon_{su,REF} \in [0.80 - 0.95]$ .

It can be seen that the reinforcement mechanism provided by the steel fibers and the inclined reinforcement reduces the stress in the reinforcement; therefore, for this study, the transverse reinforcement ratio or even the effective depth of the pile cap can be reduced. The analyses also show that the  $V_{2L,Pilecaps}/V_{2L,REF} \in$  ratio  $[1.00 - 1.65]$  indicates that, at the beginning of transverse reinforcement mobilization, the stirrups of pile caps PC02<sub>SFRC</sub>, PC03<sub>SFRC+IR</sub> and PC04<sub>IR</sub> underwent more stress than those of the reference pile cap. However, with increased loading, the fibers and the inclined reinforcement tend to assume the function of the main reinforcement. In



**Figure 13.** Final aspect of the pile caps after their failures without inclined shear reinforcement.



**Figure 14.** Final aspect of the pile caps after their failures with inclined shear reinforcement.

addition, with the imminence of failure,  $\varepsilon_{su, \text{Pilecap}} / \varepsilon_{su, \text{REF}} \in [0.80-0.95]$ , which confirms the decrease in stress in the stirrups of the pile caps with additional reinforcements (steel fiber and/or inclined reinforcement).

**Failure of pile caps.** The analysis aims to register the integrity of the pile caps after the failure of these structural elements. Figures 13 and 14 reveal the fragility of these elements and their failure mode, namely, shear by diagonal strain. P01\_REF was the weakest of all, with the least pronounced diagonal crack. The pile caps

PC03<sub>SFRC+IR</sub> and P04<sub>IR</sub> demonstrated similar behavior, presenting the formation of multiple cracks. However, comparing PC03<sub>SFRC+IR</sub> and PC02<sub>SFRC</sub>, it can be seen that the combination of inclined reinforcement and steel fibers enhances the bearing capacity, delaying the progression of cracks and inhibiting shear efforts, with the solicitation of the fibers in tension, as the load–strain and load–displacement graphs reveal. Therefore, steel fibers and shear reinforcement improved the ductility of the pile caps.

## Conclusions

The present experimental study has assessed steel fiber and inclined shear reinforcement performance in pile caps, whose variables were the use of steel fibers with and without inclined shear reinforcement. Based on the results, the following conclusions were observed:

- The use of the fibers provided the same value of the bearing capacity of the pile cap with the inclined reinforcement, with a strength gain of approximately 40%, comparing PC02<sub>SFRC</sub> and PC04<sub>IR</sub> with PC01<sub>REF</sub>.
- The fibers contributed to a 7% strength gain when the usage is combined with inclined shear reinforcement; comparing PC03<sub>SFRC+IR</sub> with PC04<sub>IR</sub>.
- The analysis of the load–displacement ratio ( $V-\delta$ ) shows that the load-bearing capacity of the pile cap with steel fibers and inclined reinforcement (PC03<sub>SFRC+IR</sub>) had the best lower displacements, 20%, and 44% reduction, respectively, compared to PC01<sub>REF</sub> and PC04<sub>I</sub>, and exhibited greater strain capacity, with  $\varepsilon_{fu}/\varepsilon_f = 1.28$ .
- Additionally, the  $V-\delta$  parameters enabled the assessment of not only strength but also the influence of steel fibers and inclined shear reinforcement on the ductility and tenacity of the pile caps. These properties increased significantly in pile caps with steel fibers and/or inclined shear reinforcement, especially PC04<sub>IR</sub>, with  $\delta_{u,Pilecaps}/\delta_{u,REF} = 1.20$  and  $T_{E,Pilecaps}/T_{E,REF} = 3.35$ .
- The load–strain graph ( $V-\varepsilon_s, IR$ ) shows that the inclined shear reinforcement of PC03<sub>SFRC+IR</sub> with hybrid composition (steel fibers + inclined shear reinforcement) did not carry yield stress.
- The mobilization of the stirrups shows that the levels of strain in the transverse reinforcements of pile caps PC02<sub>SFRC</sub>, PC03<sub>SFRC+IR</sub>, and PC04<sub>IR</sub> were lower than that of the reference pile cap. For this reason, the additional strengthening mechanisms reduced the shear efforts.
- The steel fibers restricted the strain of the inclined shear reinforcement. Therefore, it can be hypothesized that the strengthening mechanisms, under the conditions presented in this study, work satisfactorily by themselves, as the fibers tend to inhibit the action of the inclined shear reinforcement and vice versa.

## Data availability

The datasets used and/or analyzed during the current study are available from the corresponding author on reasonable request.

Received: 5 March 2022; Accepted: 7 June 2022

Published online: 16 June 2022

## References

1. ABNT NBR 6118. *Procedure: Design of Concrete Structures* (ABNT, 2014) (in Portuguese).
2. Mesquita, A. C., Rocha, A. S., Delalibera, R. G. & Silva, W. A. The influence of connecting pile cap-column in the mechanisms of break in the two pile caps. *Rev. IBRACON Estrut. Mater.* **9**, 856–882 (2016).
3. Blénot, J. Semelles en béton armé. *Annales de l'institut technique du bâtiment et des travaux publics* **10**, 111–112 (1957).
4. Blénot, J. & Frémy, R. Semelles sur pieux. *Annales de l'institut technique du bâtiment et des travaux publics* **20**, 224–273 (1967).
5. Tomaz, M. A., Delalibera, R. G., Giongo, J. S. & Gonçalves, V. F. Analysis of the nodal stresses in pile caps. *Rev. IBRACON Estrut. Mater.* **11**, 1208–1257 (2018).
6. Mobasher, B., Yao, Y. & Soranakom, C. Analytical solutions for flexural design of hybrid steel fiber reinforced concrete beams. *Eng. Struct.* **100**, 0141–0296 (2015).
7. Gomes, L. D. S. G. *et al.* Experimental analysis of the efficiency of steel fibers on shear strength of beams. *Latin Am. J. Solids Struct.* **15**, 1–16 (2018).
8. Bicelli, A. R. A., Oliveira, V. A., Matos, K. S. P. & Oliveira, D. R. C. Effects of accelerated corrosion on rebar bonding in steel fiber concrete. *Rev. Matér.* **26**, 03 (2021).
9. Moraes, M. C. *Estruturas de fundações* 169 (Editora McGraw – Hill do Brasil Ltda, 1976).
10. Delalibera, R. G. & Giongo, J. S. Numerical analysis of two pile caps with sockets embedded, subject the eccentric compression load. *Rev. IBRACON Estrut. Mater.* **16**, 436–474 (2013).
11. ABNT NBR 15530. *Specification: Steel Fibers for Concrete* (ABNT, 2019) (in Portuguese).
12. Soroushian, P. & Bayasi, Z. Fiber-type effects on the performance of steel fiber reinforced concrete. *ACI Mater. J.* **88**(2), 129–134 (1991).
13. Mahakavi, P. & Chithra, R. Impact resistance, microstructures and digital image processing on self-compacting concrete with hooked end and crimped steel fiber. *Constr. Build. Mater.* **220**, 651–666 (2019).
14. Nzambi, A. K. L. L., Oliveira, D. R. C., Oliveira, A. M. & Picanço, M. S. Pull-out tests of ribbed steel reinforcing bars embedded in concrete with steel fibres. *Proc. Inst. Civ. Eng. Struct. Build.* **174**(3), 181–189. <https://doi.org/10.1680/jstbu.17.00180> (2021).
15. ABNT NBR 7480. *Specification: Steel for the Reinforcement of Concrete Structures* (ABNT, 2007) (in Portuguese).
16. ABNT NBR ISO 6892-1. *Metallic Materials: Tensile Testing Part 1: Method of Test at Room Temperature* (ABNT, 2015) (in Portuguese).

## Acknowledgements

The authors thank the Institute of Ecological Research in the Amazon (IPEAM) for their support in the development of this study and other research in the Amazon.

### Author contributions

A.N., L.G., C.A., F.S. and D.O. made important contributions to this manuscript.

### Funding

The authors received no specific funding for this work.

### Competing interests

The authors declare no competing interests.

### Additional information

**Correspondence** and requests for materials should be addressed to A.N.

**Reprints and permissions information** is available at [www.nature.com/reprints](http://www.nature.com/reprints).

**Publisher's note** Springer Nature remains neutral with regard to jurisdictional claims in published maps and institutional affiliations.



**Open Access** This article is licensed under a Creative Commons Attribution 4.0 International License, which permits use, sharing, adaptation, distribution and reproduction in any medium or format, as long as you give appropriate credit to the original author(s) and the source, provide a link to the Creative Commons licence, and indicate if changes were made. The images or other third party material in this article are included in the article's Creative Commons licence, unless indicated otherwise in a credit line to the material. If material is not included in the article's Creative Commons licence and your intended use is not permitted by statutory regulation or exceeds the permitted use, you will need to obtain permission directly from the copyright holder. To view a copy of this licence, visit <http://creativecommons.org/licenses/by/4.0/>.

© The Author(s) 2022, corrected publication 2022